Atmospheric
Chemistry
and Physics

Supplement of

Evolution of source attributed organic aerosols and gases in a megacity of central China

Siyuan Li et al.

Correspondence to: Dantong Liu (dantongliu@zju.edu.cn) and Shaofei Kong (kongshaofei@cug.edu.cn)

Table S1: The related coefficient between OA factors, marked profiles and VOC factors.

	HOA	COA	OOA1	OOA2	NOx	BC	SO$_4^{2-}$	NO$_3^-$	Ox	Traffic VOCs	Cooking VOCs	SecVOC2	SecVOC1
HOA													
COA	0.285**												
OOA1	0.462**	0.666**											
OOA2	0.332**	-0.006	0.288**										
NOx	0.708**	0.389**	0.321**	0.088*									
BC	0.834**	0.203**	0.453**	0.504**	0.672**								
SO$_4^{2-}$	0.335	0.106**	0.294**	0.821**	0.113**	0.478**							
NO$_3^-$	0.144**	-0.068	0.039	0.435**	0.075	0.399**	0.374**						
Ox	0.344**	0.228**	0.183**	0.700**	0.310**	0.444**	0.548**	0.113**					
Traffic VOCs	0.629**	0.305**	0.409**	0.159**	0.530**	0.534**	0.219**	0.124**	0.309**				
Cooking VOCs	0.564**	0.667**	0.698**	0.065	0.561**	0.487**	0.118**	-0.034	0.271**	0.522**			
SecVOC2	0.138*	-0.076	-0.033	0.673**	0.005	0.216**	0.381**	-0.126**	0.770**	0.026*	-0.18**		
SecVOC1	0.534**	0.667**	0.758**	0.124	0.474**	0.448**	0.179**	-0.063	0.121**	0.523**	0.746**	-0.11**	

21 **Correlation is significant at the 0.01 level (two-tailed)

22 * Correlation is significant at the 0.005 level (two-tailed)

23

Text S1 PMF Analysis from HR-ToF-AMS.

The HR-ToF-AMS mass spectrometer was operated under V-mode with high sensitivity ($m/\triangle m = \sim 2000$). The relative ionization efficiencies (*RIE*s) of non-refractory species, i.e., sulfate, nitrate, chloride, and ammonium were determined to be 0.82, 1.1, 1.3, and 3.82, respectively.

The input data were the high-resolution organic mass spectral matrix of OA and the error matrix, and the Positive Matrix Factorization (PMF) analysis was conducted using the PMF Evaluation Toolkit (PET) v2.08D. A minimum error value was added to the error matrix and m/z with low signal-to-noise (SNR < 0.2) rations are removed. But, those ions with "weak" variables (0.2 < SNR < 2) are down-weighted by increasing the measurement errors by a factor of 2. The ions with m/z 19 and 20 are removed because of their negligible masses. Further, isotopes were removed since their signals are scaled to their parent ions instead of being measured directly. The number of factors in the PMF solution was explored from 1 to 6. There are several criteria that can be used to select the best modeled number of factors such as Q/Q_{exp} and the rotational parameter (*f*peak). The *f*peak parameter can analyze the rotational ambiguity of the solution sets, and it was varied from -1 to 1 by a step of 0.1. The Q-value corresponds to the number of the degrees of freedom of the fitted data: $Q_{exp} = tm - p(t + m)$, where t and m is the dimensions of the matrix, p is the number of PMF factors, and $p(t + m)$ represent the free parameters of the model. With the p increased, the Q decreased. The analysis used mass spectra consist of *m/z* 12 to 120 amu in this work. The four-factor solution with *f*peak = 0 and $Q/Q_{exp} = 3.04$ was chosen as the optimal solution according to the procedures outlined in detail elsewhereZhang et al. (2011).

Text S2 PMF Analysis from PTR-ToF-MS

The measurement error was tested based on the transmission gas and the benzene, toluene, styrene and xylenes in the exhaust. The transmission calibration provided ratios for the normalized counts per second (ncps) per ppb(Hartikainen et al., 2018). Comparison with the transmission calibrated ncps ppb^{-1} values, the measurement concentration had 20-40% uncertainty. Some reaction rates of VOCs with H_3O^+ were based on the rates by Cappellin et al.(Cappellin et al., 2012) at E/N 120, while the E/N was slightly higher (135 Td) in this experiment, which may result in underestimation of concentrations.

Positive matrix factorization (PMF 5.0) is an advanced receptor model which decomposes an observation dataset ($i \times j$ dimensions) into three matrixes including factor contributions G ($i \times k$ dimensions), profiles matrix F ($k \times j$ dimensions), and residue matrix E (e_{ij}):

$$x_{ij} = \sum_{k=1}^{p} g_{ik} f_{kj} + e_{ij} \tag{1}$$

where x_{ij} is the concentration of jth species measured in ith sample, g_{ik} is the contribution of the kth source to the ith sample, f_{kj} is the mass fraction of the jth compound in the kth source, and e_{ij} is the residual for each sample/species. The PMF solution minimizes the target function Q according to the ratio of residual matrix (e_{ij}) elements and uncertainty (U_{ij}) as:

$$Q = \sum_{i=1}^{n} \sum_{j=1}^{m} \left(\frac{e_{ij}}{U_{ij}} \right) \tag{2}$$
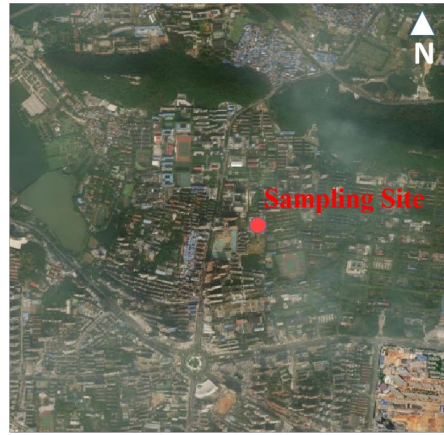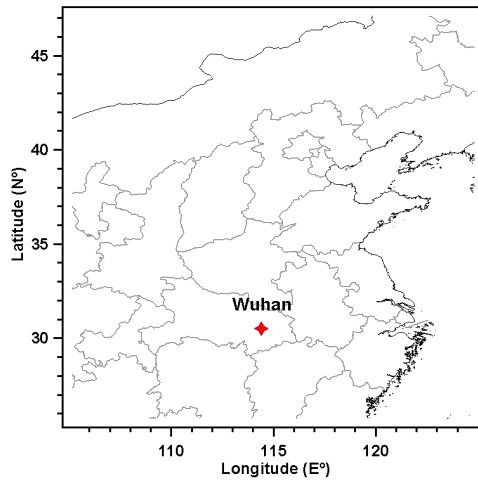
The method detection limit (MDL) and measurement uncertainties (MU%) are employed to calculate the uncertainty of each sample based on the following equations:
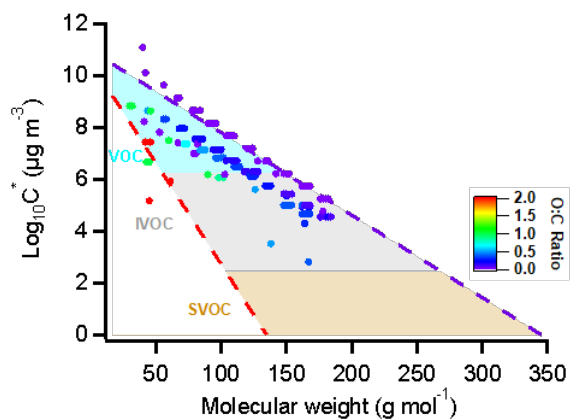
$$U_{ij} = \sqrt{(MU \times concentration)^2 + (1/2MDL)^2} \tag{3}$$

$$U_{ij} = \frac{5}{6} \times MDL \tag{4}$$

When the species concentration is higher than its MDL, Eq. (3) is used to calculate the uncertainty. Otherwise, Eq. (4) is used.

Figure S1: Location of the observation region and sampling site. (The right figure is from © Google Maps.)

Figure S2: Molecular corridors (vapor saturation pressure at 25℃, C*, as a function of molecular weight) for the compounds measured by the PTR-ToF-MS in this work, colored by the O:C ratio. Below and above logC*=6.5 and 2.5 (in μg m⁻³) is defined as intermediate-volatile and volatile organic compounds, respectively.
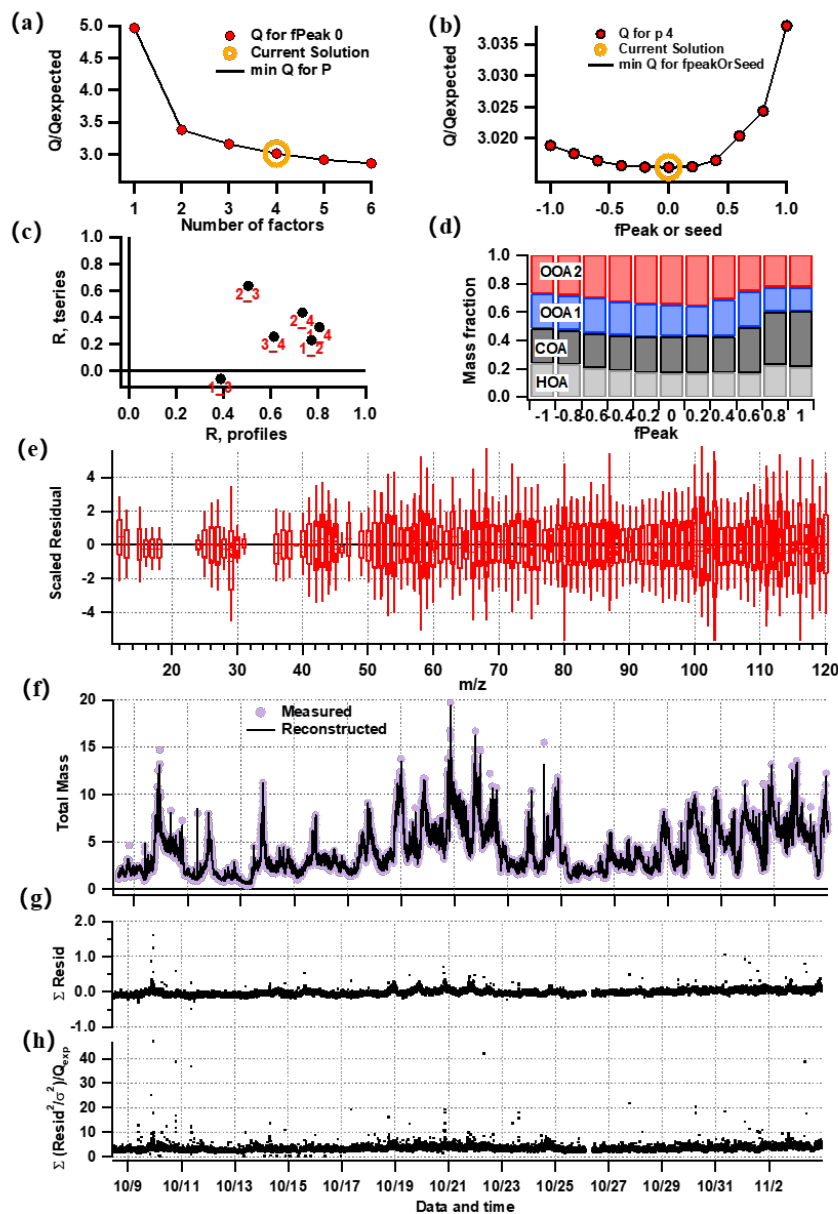
Figure S3: A summary of PMF diagnostic plot: (a) Q/Q_{exp} as a function of number of factors; (b) Q/Q_{exp} as a function of fPeak value; (c) correlations of the time series and spectral profiles among the PMF factors; (d) mass fraction of OA factors as a function of fpeak; (e) scaled residual for each fragment ion; (f) comparison of measured and PMF reconstructed mass; (g) time series of residual, and (h) time series of Q/Q_{exp} values.
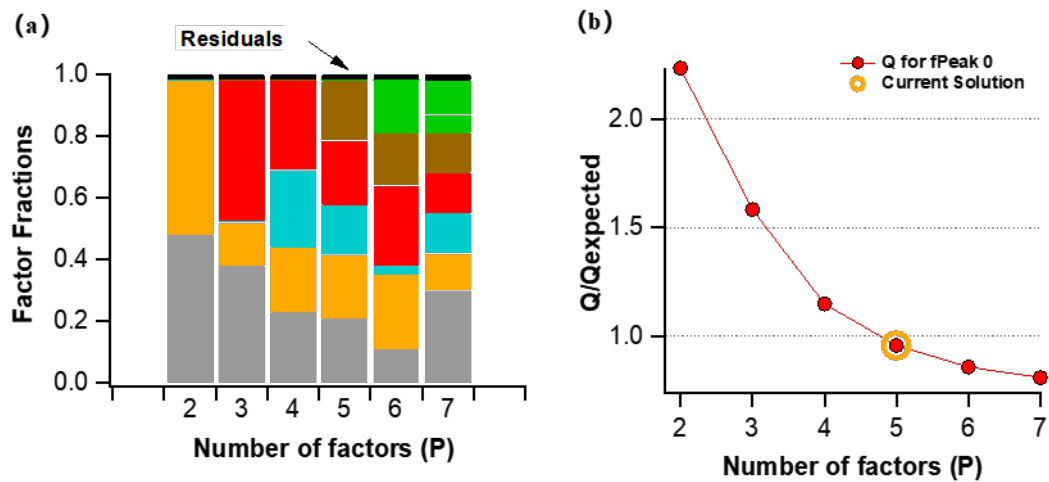
Figure S4: Q/Q_{exp} **values as a function of factor number in PMF (a); factor fractions from various factors in different PMF solutions (b).**
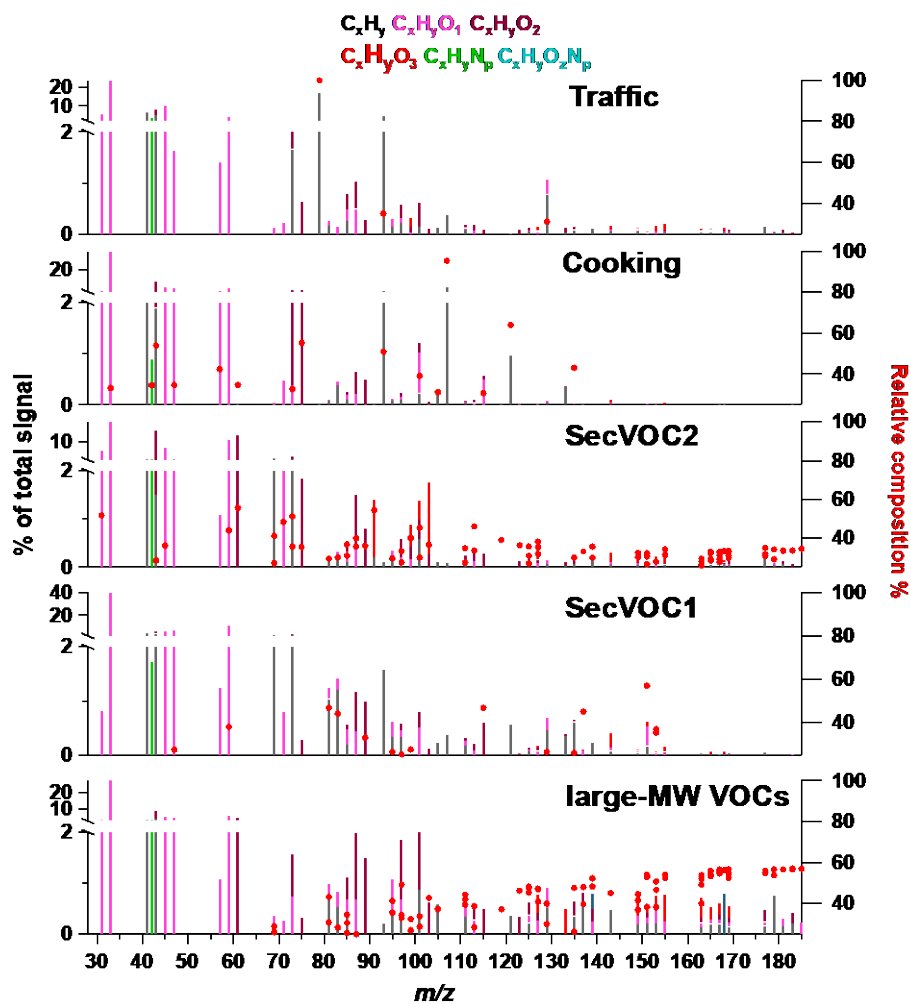
84
85 **Figure S5: Source attributed VOCs measured by the PTR-TOF-MS (a-e). Mass profiles of the five factors resolved of**
86 **PMF (traffic VOCs, cooking VOCs, secondary VOCs (SecVOC2, SecVOC1) and large molecular weight (MW) VOCs**
87 **(large-MW VOCs), with major relative composition contribution labeled in the mass spectra.**
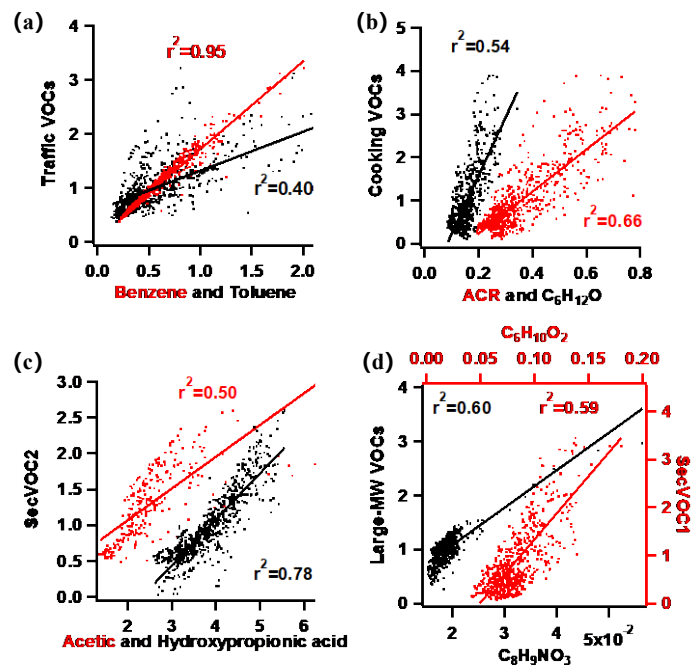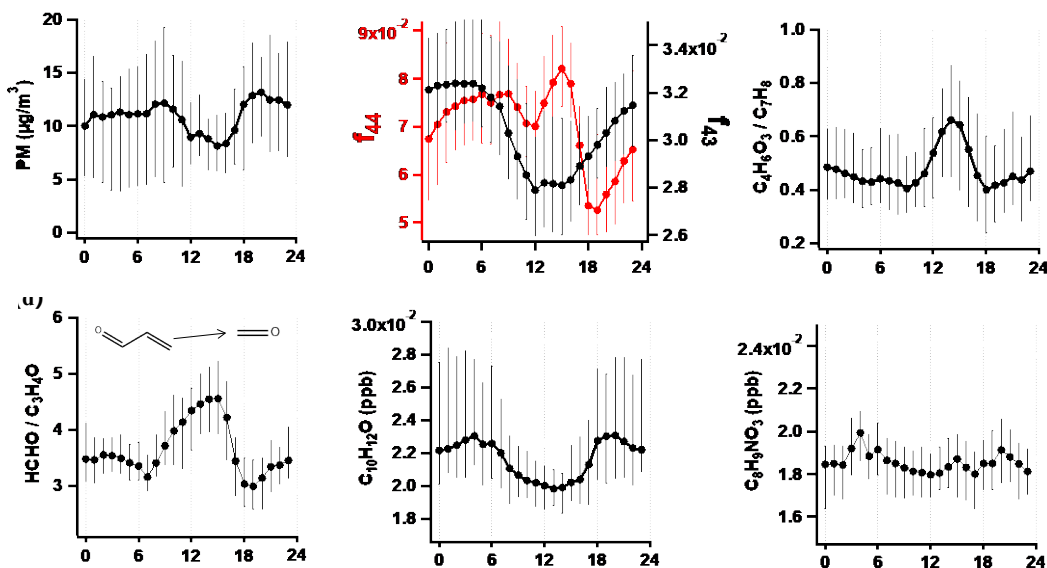88
89

Figure S6: The scatter plots between VOCs factors and tracer species (ppb).
93

Figure S7: Diurnal variations of: (a) total PM concentration measured by SMPS; (b) f_{44} (left) and f_{43} (right); (c-f) involved species both during photo- and dark oxidation.

References

Cappellin, L., Karl, T., Probst, M., Ismailova, O., Winkler, P., Soukoulis, C., Aprea, E., Märk, T., Gasperi, F., and Biasioli, F.: On Quantitative Determination of Volatile Organic Compound Concentrations Using Proton Transfer Reaction Time-of-Flight Mass Spectrometry, Environ. Sci. Technol., 46, 2283-2290, https://doi.org/10.1021/es203985t, 2012.

Hartikainen, A., Yli-Pirilä, P., Tiitta, P., Leskinen, A., Kortelainen, M., Orasche, J., Schnelle-Kreis, J., Lehtinen, K., Zimmermann, R., Jokiniemi, J., and Sippula, O.: Volatile Organic Compounds from Logwood Combustion: Emissions and Transformation under Dark and Photochemical Aging Conditions in a Smog Chamber, Environ. Sci. Technol., 52, 4979–4988, https://doi.org/10.1021/acs.est.7b06269, 2018.

Zhang, Q., Jimenez, J., Canagaratna, M., Ulbrich, I., Ng, N., Worsnop, D., and Sun, Y.: Understanding atmospheric organic aerosols via factor analysis of aerosol mass spectrometry: a review, Anal. Bioanal. Chem., 401, 3045-3067, https://doi.org/10.1007/s00216-011-5355-y, 2011.